

# MeO-Biphep and Binap Ligands as Six-Electron Donors to Ruthenium(II). X-ray and NMR Studies on Cp-, Pyrrole-, and Indole-Derived Complexes

Nantko Feiken, Paul S. Pregosin,\* and Gerald Trabesinger

Laboratorium für Anorganische Chemie, ETH Zentrum, 8092 Zürich, Switzerland

Alberto Albinati\* and Giacomo L. Evoli

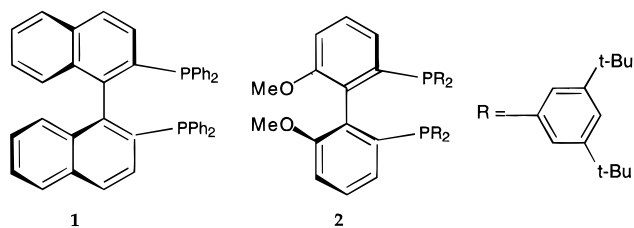
Chemical Pharmacy, University of Milan, I-20131 Milan, Italy

Received August 18, 1997<sup>®</sup>

Ru(II) complexes of the chiral ligands Binap and MeO-Biphep containing six-electron hydrocarbon donors, such as Cp, a deprotonated pyrrole, or the benzene ring of indole, attain the 18-electron configuration by complexing a proximate biaryl double bond. The solid-state structures for two of these, [RuCp(2)]BF<sub>4</sub> and [Ru(indole)(2)](BF<sub>4</sub>)<sub>2</sub> (2 = (6,6'-dimethoxybiphenyl-2,2'-diyl)bis(bis(3,5-di-*tert*-butylphenyl)phosphine)), have been determined by X-ray diffraction. They reveal that a biaryl double bond, immediately adjacent to one P-donor, coordinates to the ruthenium, thus making the chelating ligand a six-electron donor. The double bonds remain coordinated in solution as shown by HMBC <sup>13</sup>C, <sup>1</sup>H long-range correlation spectroscopy. However, 2-D NMR exchange spectroscopy suggests that the biaryl double bond is weakly coordinated since the two halves of the C<sub>2</sub>-symmetric Binap (or MeO-Biphep) ligands are in slow exchange at ambient temperature.

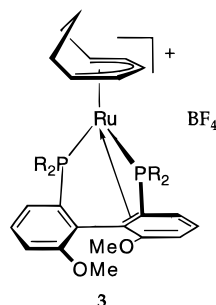
## Introduction

New applications in organic synthesis involving chiral bidentate phosphine complexes in connection with enantioselective homogeneous catalysis now appear regularly.<sup>1</sup> Although there are many useful and commercially available chiral ligands, the atropisomeric class, which includes Binap<sup>2</sup> (1) and MeO-Biphep<sup>3</sup> (specifically 2<sup>4,5</sup>), has proven immensely successful.



We have recently shown<sup>4</sup> that Ru(II) complexes of 2 are capable of coordinating one of the biaryl double

bonds, e.g., in the pentadienyl complex, 3. This bonding



mode was somewhat unexpected, so that we have considered additional Ru(II) complexes of both 1 and 2 to determine whether the bonding in 3 was an oddity or whether this capability could be extended to a wider variety of compounds. The 16-electron five-coordinate hydrido cation [RuH(2)(isopropyl alcohol)<sub>2</sub>]<sup>+</sup> does not show this type of bonding.<sup>5</sup> We report here on the Binap complexes 4 and 5 as well as on the MeO-Biphep complexes 6–8 (see Scheme 1), all of which show this novel type of η<sup>4</sup>-coordination mode.

## Results and Discussion

**Solid-State Structures.** The solid-state structures of the MeO-Biphep complexes 7 and 8 with coordinated η<sup>5</sup>-Cp and η<sup>6</sup>-indole ligands, respectively, were determined by X-ray diffraction methods, and several views for these complexes are shown in Figures 1 and 2. The local coordination spheres of both complexes consist of

<sup>®</sup> Abstract published in *Advance ACS Abstracts*, December 1, 1997.

(1) *Organic Synthesis via Organometallics OSM 5*; Helmchen, G., Dibo, J., Flubacher, D., Wiese, B., Eds.; Vieweg: Braunschweig/Wiesbaden, 1997. Trost, B. *Angew. Chem.* **1995**, *107*, 285. Hayashi, T. In *Catalytic Asymmetric Synthesis*; Ojima, I., Ed.; VCH Publishers, Inc.: New York, 1993; p 325. Brown, J. M.; *Chem. Soc. Rev.* **1993**, 25.

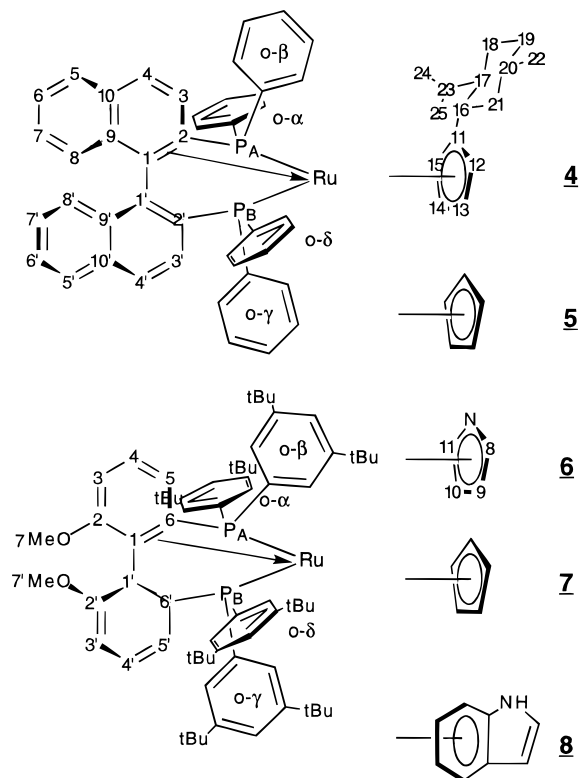
(2) Kitamura, M.; Noyori, R. *Mod. Synth. Meth.* **1989**, *5*, 116. Ohta, T.; Tonomura, Y.; Nozaki, K.; Takaya, H.; Mashima, K. *Organometallics* **1996**, *15*, 1521. Zhang, X.; Uemura, T.; Matsumura, K.; Sayo, N.; Kumabayashi, H.; Takaya, H. *Synlett* **1994**, 501. Kitamura, M.; Tokunaga, M.; Noyori, R. *J. Am. Chem. Soc.* **1993**, *115*, 144. Ohta, T.; Miyake, T.; Seido, N.; Kumabayashi, H.; Akutagawa, S.; Takaya, H. *Tetrahedron Lett.* **1992**, *33*, 635. Mashima, K.; Hino, T.; Takaya, H. *J. Chem. Soc., Dalton Trans.* **1992**, 2099. Ohta, T.; Takaya, H.; Noyori, R. *Inorg. Chem.* **1988**, *27*, 566.

(3) Schmid, R.; Broger, E. A.; Cereghetti, M.; Cramer, Y.; Foricher, J.; Lalonde, M.; Mueller, R. K.; Scalone, M.; Schoettel, G.; Zutter, U. *Pure Appl. Chem.* **1996**, *68*, 131. Heiser, B.; Broger, E. A.; Cramer, Y. *Tetrahedron: Asymmetry* **1991**, *2*, 51. Schmid, R.; Foricher, J.; Cereghetti, M.; Schoenholzer, P. *Helv. Chim. Acta* **1991**, *74*, 370. Mezzetti, A.; Tschumper, A.; Consiglio, G. *J. Chem. Soc., Dalton Trans.* **1995**, 49. Mezzetti, A.; Costella, L.; Del Zotto, A.; Rigo, P.; Consiglio, G. *Gazz. Chim. Ital.* **1993**, *123*, 155.

(4) (a) Feiken, N.; Pregosin, P. S.; Trabesinger, G. *Organometallics* **1997**, *16*, 537. (b) *Organic Synthesis via Organometallics OSM 5*; Helmchen, G., Dibo, J., Flubacher, D., Wiese, B., Eds.; Vieweg: Braunschweig/Wiesbaden, 1997; p 155.

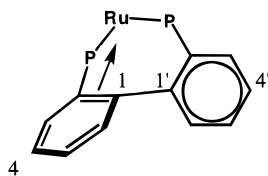
(5) Currao, A.; Feiken, N.; Macchioni, A.; Nesper, R.; Pregosin, P. S.; Trabesinger, G. *Helv. Chim. Acta* **1996**, *79*, 1587.

## Scheme 1. Numbering System for the Complexes



the chiral six-electron phosphine donor (two P atoms and the aryl double bond) plus the Cp or indole hydrocarbons. In compound **7**, the usual  $\eta^5$ -Cp coordination mode is found, with all five carbons ca. equidistant from the ruthenium. In the dicationic indole complex **8**, the benzene ring of the indole is complexed.

Inspection of both structures reveals that the coordination of the aryl double bond is facilitated by a distortion of the biaryl moiety. Normally, the two biaryl rings would be ca. perpendicular and thus the angle made by the two lines connecting C1 and C4 and C1' and C4' would be ca.  $0^\circ$ ; however, in both complexes, the biaryl bends such that the angle between these two lines is ca.  $20^\circ$  in **7** and ca.  $34^\circ$  in **8**, thus making the the  $\pi$ -system of the coordinated double bond more accessible to the metal.



Nevertheless, the Ru–C1 and Ru–C6 bond lengths are relatively long and lie between ca. 2.31 and 2.38 Å. In the cationic hydrido–styrene complex  $[\text{RuH}(\text{PhCH}=\text{CH}_2)(\eta^6\text{-cymene})(\text{PPh}_3)]^+$ , Faller and co-workers<sup>6</sup> find Ru–C separations for the styrene of 2.195(6) and 2.216(6) Å. Similarly, for the cationic hydrido–ethylene derivative  $[\text{RuH}(\text{C}_2\text{H}_4)(\text{C}_6\text{Me}_6)(\text{PPh}_3)]^+$ , Werner and co-workers<sup>7</sup> report Ru–C values of 2.168(10) and 2.194(9) Å for the complexed ethylene.

(6) Faller, J. W.; Chase, K. J. *Organometallics* **1995**, *14*, 1592.  
(7) Kletzin, H.; Werner, H.; Serhadli, O.; Ziegler, M. L. *Angew. Chem.* **1983**, *95*, 49.

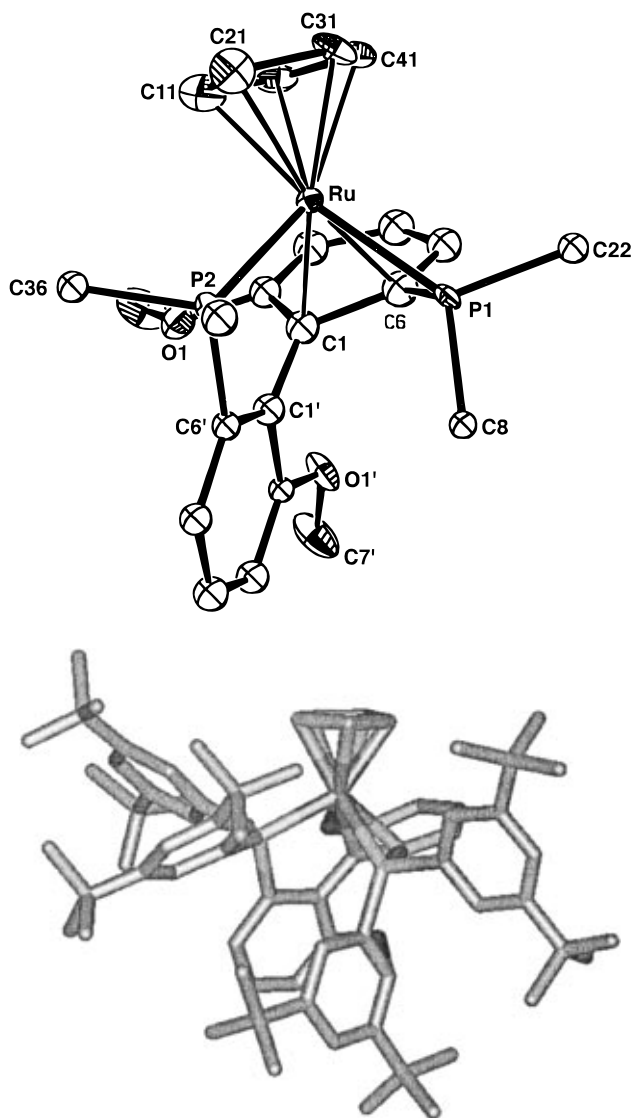
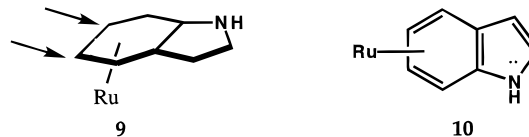


**Figure 1.** (a) ORTEP plot for a part of the cationic Cp complex **7**. (b) View<sup>22</sup> of the entire cation.

There is an obvious tilt of the plane of the coordinated indole in **8** relative to the plane defined by the metal and the two P donors (see Figure 2). This is sufficiently marked such that the six aromatic carbons are not all equally separated from the metal atom. The carbons with the two shortest distances are indicated by the arrows in **9**.



Obviously, this distortion could be steric in origin; however, there are no close contacts between the various organic fragments of the chiral phosphine and the indole. Possibly, this dicationic complex is distorting toward an  $\eta^4$  16-electron species, i.e., **10**. This would allow the five-membered ring to retain aromaticity. Unfortunately, the large experimental uncertainties do not allow an exact analysis of the various Ru–C distances. DuBois and co-workers<sup>8</sup> have found a similar tilt of the coordinated indolyl ligand in  $[\text{Ru}(\eta^6\text{-2,3-dimethylindolyl})(\eta^6\text{-cymene})](\text{BPh}_4)$ , in which the NH is

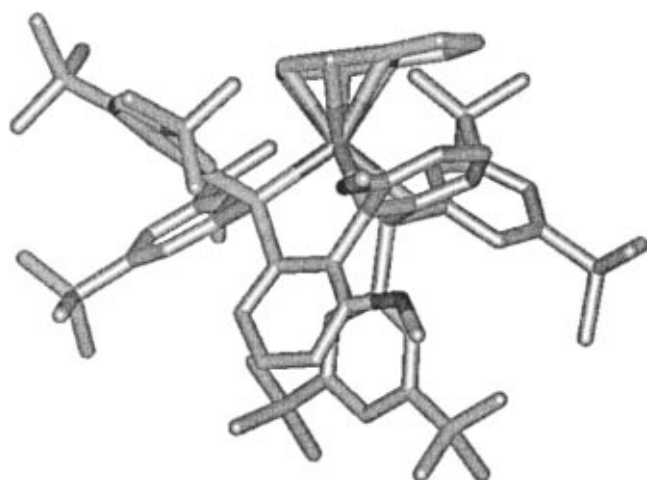
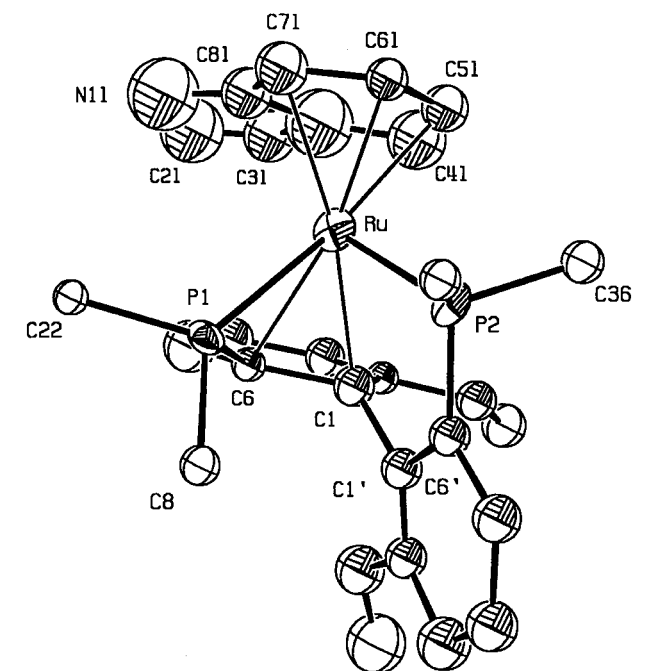


**Figure 2.** (a) ORTEP plot for the dicationic indole complex **8**. (b) View<sup>22</sup> of the entire dication.

deprotonated. They have also reported<sup>9</sup> the solid-state structure for the dication  $[\text{Ru}(\eta^6\text{-1-Me-indoline})(\eta^6\text{-cymene})](\text{OTf})_2$ .

As a consequence of the coordination of the biaryl double-bond in **7** and **8**, one observes very different angles about the two P atoms (see Table 1). For the Ru–P1–C6 angles in these compounds, the values are ca. 66° and 68°, respectively, due to the additional olefin complexation. However, for Ru–P2–C6', we find the more routine values of ca. 107° and 106°, respectively.

It is interesting to compare the observed structures of **2** in **7** and **8** (see Figure 3) with that found for **2** in  $[\text{RuH}(\text{p-cymene})(\mathbf{2})]^+$ ,<sup>10</sup> which has a conventional MeO-Biphep bidentate coordination mode. In the latter, we observe the now classical pseudo-axial and pseudo-equatorial arrangement of the P–phenyl groups; however, in **7** and **8**, three of the P–phenyl groups now

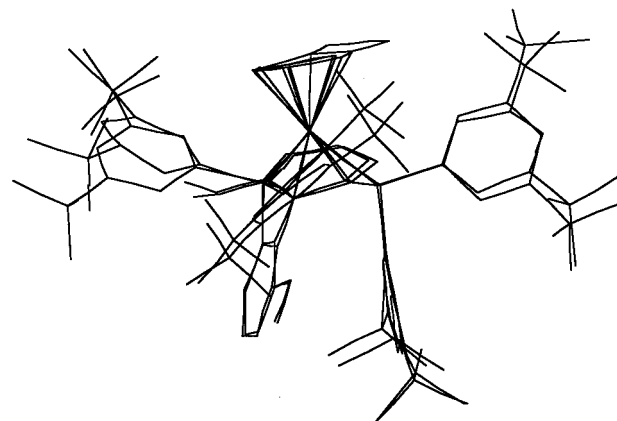


**Figure 3.** Comparison<sup>23</sup> of the structures of **7** and **8** showing that the benzene ring of the complexed indole in **8** occupies almost the same position as the Cp ligand in **7**. Moreover, there is no longer a set of pseudo-axial and pseudo-equatorial P–aryl ring substituents.

**Table 1.** Bond Lengths (Å) and Bond Angles (deg) for **7** and **8**

	L = Cp, <b>7</b>		L = indole, <b>8</b>
Ru–P1	2.317(4)	Ru–P1	2.315(7)
Ru–P2	2.273(4)	Ru–P2	2.287(7)
Ru–C1	2.38(1)	Ru–C1	2.34(3)
Ru–C6	2.31(1)	Ru–C6	2.31(3)
Ru–C1L	2.19(2)	Ru–C4L	2.36(4)
Ru–C2L	2.19(2)	Ru–C5L	2.27(3)
Ru–C3L	2.21(1)	Ru–C6L	2.15(3)
Ru–C4L	2.23(1)	Ru–C7L	2.26(3)
Ru–C5L	2.23(1)	Ru–C8L	2.41(3)
		Ru–C9L	2.44(4)
P1–Ru–P2	93.5(1)	P1–Ru–P2	91.0(3)
P1–Ru–C1	72.3(4)	P1–Ru–C1	71.7(7)
P1–Ru–C6	47.1(4)	P1–Ru–C6	44.0(6)
Ru–P1–C6	66.2(5)	Ru–P1–C6	67.8(9)
Ru–P1–C22	123.7(4)	Ru–P1–C22	122.7(9)
Ru–P2–C6'	107.0(5)	Ru–P2–C6'	106.4(10)
Ru–P2–C36	118.2(5)	Ru–P2–C36	113.4(9)
Ru–P2–C50	117.0(5)	Ru–P2–C50	118.7(8)

occupy more pseudo-equatorial-like positions. From Figure 3, one also sees that the coordinated benzene ring of **8** occupies essentially the same space as the Cp ligand in **7** and that there are no unexpected steric effects disturbing the coordination of the indole ligand.

The four Ru–P separations (ca 2.27–2.32 Å) as well as the 12 P–C bond lengths (ca 1.77–1.86 Å) in **7** and **8** are relatively routine.<sup>11</sup> The observed P–Ru–P bond angles of 93.5(1)° and 91.0(3)°, respectively, suggest no special strain and fall within the expected range for MeO-Biphep complexes, e.g.,  $[\text{RuH}(\text{isopropyl alcohol})_2(\mathbf{2})]^+ = 91.0(3)^\circ$ ,<sup>5</sup>  $[\text{RuH}(\text{p-cymene})(\mathbf{2})]^+ = 91.1(6)^\circ$ ,<sup>10</sup>  $[\text{Ru}(\eta^5\text{-C}_8\text{H}_{11})(\mathbf{2})] = 96.9(1)^\circ$ .<sup>4a</sup>

**Solution Studies on the Cp Complexes.** Given that the biaryl double bond coordination in this MeO-Biphep series seems to have some generality, it was of interest to compare the solution characteristics of related Binap and Biphep derivatives. The solid-state

(8) Chen, S.; Carperos, B.; Noll, B.; Swope, J.; Dubois, M. R. *Organometallics* **1995**, *14*, 1221.

(9) Chen, S.; Vasquez, L.; Noll, B. C.; Dubois, M. R. *Organometallics* **1997**, *16*, 175.

(10) Trabesinger, G.; Albinati, A.; Feiken, N.; Kunz, R. W.; Pregosin, P. S.; Tschoerner, M. *J. Am. Chem. Soc.* **1997**, *119*, 6315.

(11) (a) DuBois, M. R.; Parker, K. G.; Ohman, C.; Noll, B. C. *Organometallics* **1997**, *16*, 2325. (b) Gao, J.; Ikariya, T.; Noyori, R. *Organometallics* **1996**, *15*, 1087. (c) Zanetti, N. C.; Spindler, F.; Spencer, J.; Togni, A.; Rihs, G. *Organometallics* **1996**, *15*, 860. (d) Mudalige, D. C.; Rettig, S. J.; James, B. R.; Cullen, W. R. *J. Chem. Soc., Chem. Commun.* **1993**, 830. (e) Cashman, R. S. M.; Butler, I. R.; Cullen, W. R.; James, B. R.; Charland, B. J. P.; Simpson, J. *Inorg. Chem.* **1992**, *31*, 5509.

Table 2. Selected NMR Data<sup>a</sup> for Complexes 4–7

4 <sup>c,e</sup>			5 <sup>b,e</sup>			6 <sup>b,d</sup>			7 <sup>b,d</sup>		
<sup>1</sup> H	<sup>13</sup> C	<sup>31</sup> P	<sup>1</sup> H	<sup>13</sup> C	<sup>31</sup> P	<sup>1</sup> H	<sup>13</sup> C	<sup>31</sup> P	<sup>1</sup> H	<sup>13</sup> C	<sup>31</sup> P
2	55.0		2	56.9		6	69.7		6	66.4	
1	87.4		1	88.2		1	88.6		1	86.5	
11	117.7		Cp	4.40	88.3	8	6.48	104.5	Cp	4.13	86.8
12	4.82	82.2				9	3.79	88.2			
13	4.31	84.5				10	4.66	84.9			
14	4.04	90.7				11	3.92	118.7			
15	3.29	88.4									
P <sub>A</sub>		5.2	P <sub>A</sub>		14.9	P <sub>A</sub>		8.2	P <sub>A</sub>		8.2
P <sub>B</sub>		75.0	P <sub>B</sub>		74.9	P <sub>B</sub>		81.9	P <sub>B</sub>		79.4
<sup>2</sup> J		44	<sup>2</sup> J		43.9	<sup>2</sup> J		45.8	<sup>2</sup> J		47.1

<sup>a</sup> Chemical shifts in ppm, coupling constants in Hertz, CD<sub>2</sub>Cl<sub>2</sub> solutions. <sup>b</sup> 293 K. <sup>c</sup> 243 K. <sup>d</sup> 400 MHz. <sup>e</sup> 500 MHz.

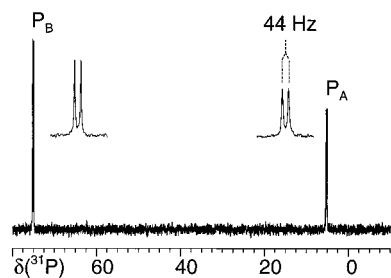


**Figure 4.** <sup>31</sup>P spectrum for **4** revealing the low-frequency shift of P<sub>A</sub> due to the η<sup>6</sup>-bonding mode of the Binap ligand (CD<sub>2</sub>Cl<sub>2</sub>, 243 K, 500 MHz).

structure of [Ru(Cp)(Binap)]<sup>+</sup>, **5**, is known,<sup>12</sup> and samples of this and the neomenthyl Cp-substituted analog, **4**, were available.<sup>13</sup>

The appropriate one- and two-dimensional NMR spectra for these compounds, **4**, **5**, and **7**, were obtained. Figure 4 shows the <sup>31</sup>P spectrum for the neomenthyl-Cp derivative **4** and reveals an AX spin pattern (δ = 75.0 and 5.2, <sup>2</sup>J(P,P) = 44 Hz), with one of the two phosphorus spins resonating at very low frequency (the <sup>31</sup>P spectrum for the Cp derivative is qualitatively the same, see Table 2). This unexpected low-frequency resonance is now recognized<sup>4,12</sup> to be typical of this η<sup>4</sup>-bonding mode and can be assigned to the P donor proximate to the coordinated olefin.

Figure 5 shows the long-range C,H correlation for the cation [RuCp(Binap)]<sup>+</sup>. One finds cross peaks stemming from the two- and three-bond J(C,H) coupling constants, which pinpoint the positions of the *very difficult to observe* <sup>13</sup>C signals<sup>14</sup> arising from the coordinated biaryl double bond. The C2 resonance correlates to the protons at C3 and C4; whereas the C1 signal shows cross peaks from the protons of C3 and C8. In all three derivatives, **4**, **5**, and **7**, these <sup>13</sup>C resonances are shifted markedly to low frequency, in keeping with the literature<sup>15</sup> for a coordinated double bond. For [RuCp(Binap)]<sup>+</sup>, the C1 resonance lies *under* the Cp signal. A summary of the

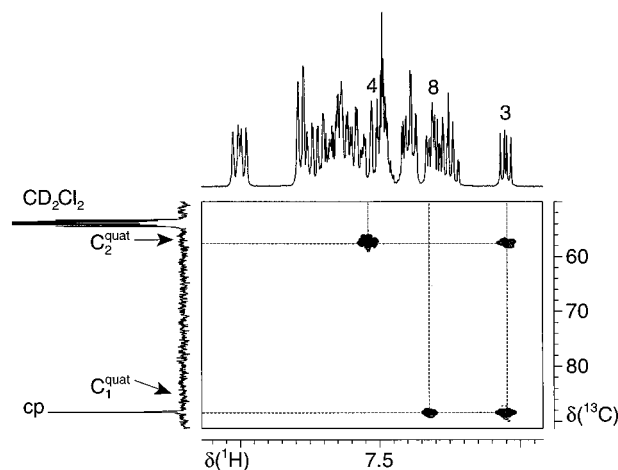
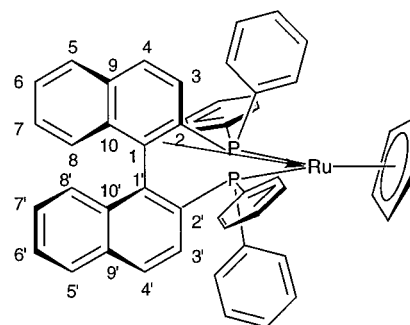


**Figure 5.** C,H long-range correlation for **5** showing the cross peaks due to the two biaryl carbons which coordinate to Ru(II) (CD<sub>2</sub>Cl<sub>2</sub>, 293 K, 400 MHz). For these complexes it is normal that the biaryl carbons have long T<sub>1</sub>'s. C1 lies under the Cp.

pertinent NMR data for these three complexes is also given in Table 2. From both the solid- and solution-state data, it is clear that the Binap and MeO-Biphep ligands are capable of this type of biaryl double-bond bonding in these Cp complexes.

Figure 6 shows the proton 2-D exchange spectrum<sup>16</sup> for the cation [RuCp(Binap)]<sup>+</sup>. Analysis of the spectrum shows that the two halves of the chiral auxiliary are

(12) Pathak, D. D.; Adams, H.; Bailey, N. A.; King, P. J.; White, C. *J. Organomet. Chem.* **1994**, *479*, 237.

(13) We thank Dr. Colin White, University of Sheffield, for the generous gift of these two Binap complexes.

(14) These fully substituted aromatic carbons have long spin-lattice relaxation times. C1 does not even have a geminal proton to assist the dipole-dipole relaxation. Consequently, we rarely observe this resonance in the conventional 1-D <sup>13</sup>C spectrum. Fortunately, the intensity of the cross peaks in a 2-D C,H proton-detected correlation depends on *both* the <sup>13</sup>C and <sup>1</sup>H magnetization, so that the appropriate cross peaks are readily visible.

(15) Mann, B. E.; Taylor, B. F. *<sup>13</sup>C NMR Data for Organometallic Compounds*; Academic Press: London, 1981. Adams, C. M.; Hafner, A.; Koller, M.; Marcuzzi, A.; Prevow, R.; Solan, I.; Vincent, B.; von Philipsborn, W. *Helv. Chim. Acta* **1989**, *72*, 1658.

(16) For applications of 2-D exchange spectroscopy, see: Albinati, A.; Eckert, J.; Pregosin, P. S.; Ruegger, H.; Salzmänn, R.; Stoessel, C. *Organometallics* **1997**, *16*, 579. Barbaro, P.; Currao, A.; Herrmann, J.; Nesper, R.; Pregosin, P. S.; Salzmänn, R. *Organometallics* **1996**, *15*, 1879. Barbaro, P.; Pregosin, P. S.; Salzmänn, R.; Albinati, A.; Kunz, R. W. *Organometallics* **1995**, *14*, 5160. Herrmann, J.; Pregosin, P. S.; Salzmänn, R.; Albinati, A. *Organometallics* **1995**, *14*, 3311. Pregosin, P. S.; Salzmänn, R.; Togni, A. *Organometallics* **1995**, *14*, 842. Breutel, C.; Pregosin, P. S.; Salzmänn, R.; Togni, A. *J. Am. Chem. Soc.* **1994**, *116*, 4067. *Magn. Reson. Chem.* **1994**, *32*, 297. Lianza, F.; Macchioni, A.; Pregosin, P. S.; Ruegger, H. *Inorg. Chem.* **1994**, *33*, 4999.

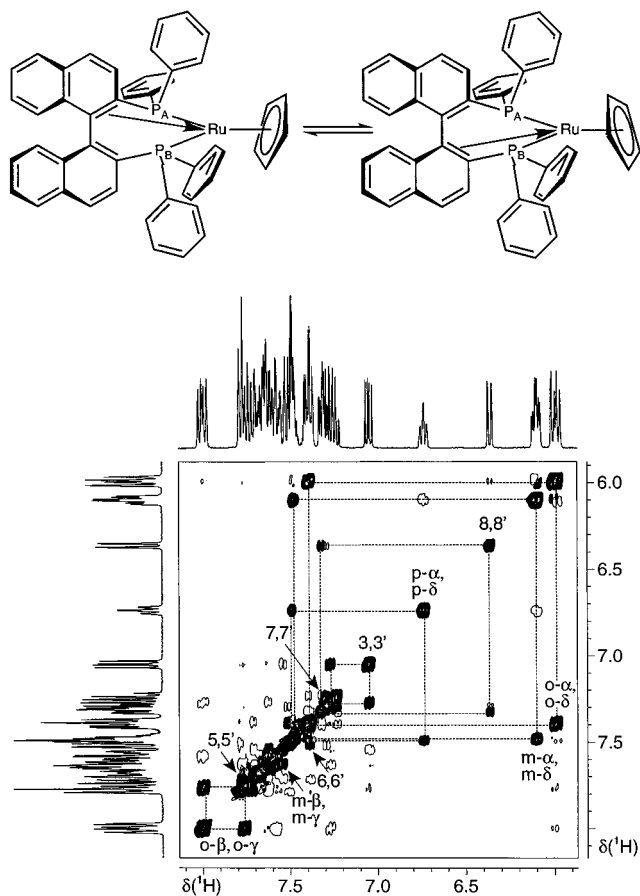


**Figure 6.** Aromatic section of the  $^1\text{H}$ -NOESY for the Binap complex **5** showing the exchange between the two halves of the  $C_2$ -symmetric ligand ( $\text{CD}_2\text{Cl}_2$ , 293 K, 400 MHz).

exchanging (e.g., 3 with 3' and 8 with 8' are clearly visible). These dynamics are consistent with the process shown in the figure and confirm that the biaryl double bond is not strongly bound to Ru (in keeping with the crystallographic bond length data) and that the metal can easily reach the 16-electron configuration by dissociating the biaryl double bond. The neomenthyl analog, **4**, shows similar dynamic behavior. We have demonstrated almost identical dynamics for the cationic  $\eta^5$ -pentadienyl complex  $[\text{Ru}(\eta^5\text{-C}_8\text{H}_{11})(\mathbf{2})]^+$ , **3**.<sup>4</sup>

The neomenthyl-Cp complex **4** is interesting in that it sheds some light on possible close contacts between a bulky Cp substituent and the Binap phenyl groups. The  $^1\text{H}$  NOESY spectrum for this complex at ambient temperature (lower trace of Figure 7) shows *random* contacts between the four Cp spins, 12–15, and the Binap ortho P-phenyl protons, i.e., the Cp moiety rotates fairly freely, thus allowing these protons to periodically approach the different Binap sites. At 243 K (upper trace), the rotation is relatively slow and the contacts to these same ortho P-phenyl protons, are much more selective, e.g., H12 now shows relatively strong NOEs to the *o*- $\alpha$  and *o*- $\delta$  protons, but H14 reveals little or no NOE contacts to these Binap aryl protons. Furthermore, the aliphatic methine proton, immediately adjacent to the Cp ring (not shown in the figure), shows only one strong contact to the ortho protons of the  $\alpha$  ring. These NOE data suggest that in a hypothetical enantioselective reaction involving this neomenthyl Cp ligand, the transfer of chiral information from Binap would be more efficient at low temperature.

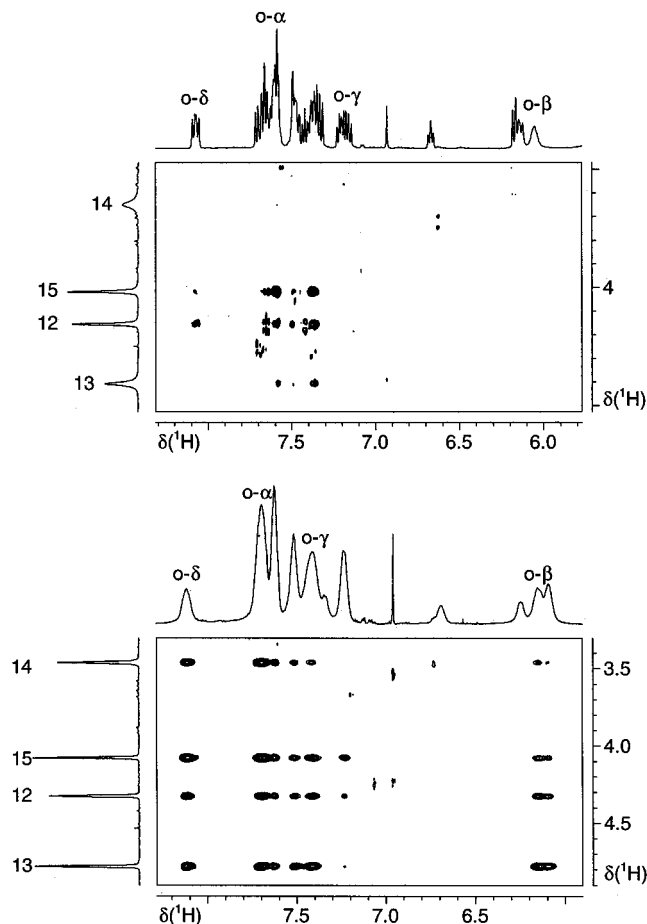
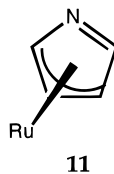


**Figure 7.** ROESY ( $\text{CD}_2\text{Cl}_2$ , 243 K, 500 MHz) and NOESY for **4** ( $\text{CD}_2\text{Cl}_2$ , 300 K, 500 MHz) showing the (+)-neomenthyl-Cp protons versus the aromatic protons. At 300 K (bottom), all ortho protons for the  $\alpha$ ,  $\beta$ ,  $\gamma$ , and  $\delta$  rings show interactions to all the Cp, reflecting the free rotation of (+)-neomenthyl-Cp protons at 300 K. The broadened aromatic resonances is consistent with this rotation. At 243 K (top), the NOEs now reflect one well-defined position of (+)-neomenthyl-Cp with respect to the BINAP ligand. Protons 13 and 14 are broader due to slow rotation of the (+)-neomenthyl moiety around the Ru-Cp axis.

**Solution Studies on the Pyrrole and Indole Complexes.** The MeO-Biphep deprotonated pyrrole derivative **6** shows NMR characteristics which are similar to those for its Cp analog **7**, see Table 2. The biaryl double bond is coordinated ( $\delta$  C1 = 88.6 and  $\delta$  C6 = 69.7), and the complex shows one of the two  $^{31}\text{P}$  signals at low frequency ( $\delta$  = 81.9 and 8.2,  $^2J(\text{P},\text{P})$  = 45.8 Hz). Interestingly, the four  $^{13}\text{C}$  signals from the deprotonated pyrrole, C8–C11, are all different:  $\delta$  = 104.5, 88.2, 84.9, and 118.7, respectively. In uncomplexed pyrrole, the C2 and C3 carbons resonate at  $\delta$  ca. 117.3 and 107.6 ppm, respectively. Although the free ligand is a poor model for **6**, there are recent studies on  $\eta^5$ -pyrrolyl<sup>11a</sup> and  $\eta^5$ -methyl-substituted pyrrolyl<sup>17</sup> Ru complexes. For  $\text{RuH}(\eta^5\text{-pyrrolyl})(\text{PPh}_3)_2$  and  $\text{RuI}(\eta^5\text{-pyrrolyl})(\text{PPh}_3)_2$ , one observes  $^{13}\text{C}$  signals at 110.0, 82.0 and 107.4, 84.3 ppm, respectively, for the  $\alpha$  and  $\beta$  pyrrolyl carbons in these complexes.<sup>11a</sup> Consequently, the observed difference between the two  $^{13}\text{C}$  signals adjacent to nitrogen in **6** (104.5 and 118.7 ppm) is somewhat of a surprise. Assuming the now established  $\eta^5$ -bonding mode<sup>11a,17</sup> for this fairly small ligand, one would not expect marked steric effects. Perhaps the  $\eta^5$ -pyrrolyl

is leaning toward an  $\eta^3$  mode, i.e., as shown in **11**; however, without an accurate solid-state structure, this is rather speculative.



In solution, the indole compound **8** shows at least three different complexes so that a detailed analysis of its solution properties was not undertaken.  $^{31}\text{P}$  NMR suggests that two of these have the  $\eta^4$ -bonding mode. Most probably, these two  $\eta^4$ -compounds differ in the position of the indole five-membered ring with respect to the  $\eta^4$ -Biphep ligand. The third complex shows a very broad doublet at ca. 67 ppm and has not been identified. We also know from a natural abundance HMQC  $^{15}\text{N}$  spectrum that all three species retain the N–H bond based on their very similar  $^{15}\text{N}$  chemical shifts. Nevertheless, the complexity of the  $^1\text{H}$  NMR spectrum resulting from this mixture prohibits further structural discussion.

In summary, the bidentate ligands in complexes **4–8**, all reveal the  $\eta^4$  six-electron-donor bonding mode. Obviously, there is nothing special in the *tert*-butyl MeO-Biphep ligand **2** since Binap readily produces the same type of bonding. Both **5** and **7** have similar dynamics in solution, confirming that the Ru(II) center should be able to take up new ligands by dissociating the biaryl double bond.

## Experimental Section

**General.** All reactions were performed in an atmosphere of Ar using standard Schlenk techniques. Dry and oxygen-free solvents were used.  $\text{Ru}(\text{OAc})_2$  **2** was provided by F. Hoffman-La Roche, Basel. Routine  $^1\text{H}$  (300.13 MHz) and  $^{31}\text{P}$  (121.5 MHz) NMR spectra were recorded with a Bruker DPX-300 spectrometer.  $^{19}\text{F}$  (188.3 MHz) NMR spectra were recorded with a Bruker AC200 spectrometer. The two-dimensional studies were carried out at using either 400 or 500 MHz for  $^1\text{H}$ . Chemical shifts are given in ppm, and coupling constants ( $J$ ) are given in Hertz. IR spectra were recorded with a Perkin-Elmer 882 infrared spectrophotometer. Elemental analyses and mass spectroscopic studies were performed by the ETHZ analytical facility.

**Crystallography.** Crystals of **7** and **8** suitable for X-ray diffraction were obtained from THF/hexane. For **8**, it was only possible to obtain crystals of poor quality and diffracting power. Crystals of both compounds, mounted on glass fibers, were cooled to 200 and 190 K, respectively, by using an Enraf-Nonius FR558SH nitrogen gas-stream cryostat installed on the CAD4 diffractometer, which was used for the space group determination and for the data collection. Unit cell dimensions were obtained by least-squares fit of the  $2\theta$  values of 25 high-order reflections. Crystallographic and other relevant data are listed in Table 3 and Supporting Information Table S1. Data were measured with variable scan speed to ensure constant statistical precision on the collected intensities. Three standard reflections were used to check the stability of the crystals and of the experimental conditions and were measured every hour. The collected intensities were corrected for Lorentz and polarization factors.<sup>18</sup>

(17) Kvietok, F.; Carperos, A. V.; DuBois, M. R. *Organometallics* **1994**, *13*, 60.

**Table 3. Experimental Data for the X-ray Study of **7** and **8****

compound	<b>7</b>	<b>8</b>
formula	$\text{C}_{75}\text{H}_{110}\text{BF}_4\text{O}_2\text{P}_2\text{Ru}$	$\text{C}_{78}\text{H}_{102}\text{B}_2\text{F}_8\text{NO}_2\text{P}_2\text{Ru}$
mol wt	1284.46	1422.43
data collection $T$ , K	200	190
cryst syst	orthorhombic	orthorhombic
space group	$P2_12_12_1$	$P2_12_12_1$
$a$ , Å	14.577 (9)	15.622 (9)
$b$ , Å	18.846 (8)	18.216 (6)
$c$ , Å	28.433 (10)	28.616 (8)
$V$ , Å <sup>3</sup>	7811 (7)	8143 (8)
$Z$	4	4
$\rho$ (calcd), g cm <sup>-3</sup>	1.092	1.160
$\mu$ , cm <sup>-1</sup>	2.827	2.838
radiation	Mo K $\alpha$ (graphite monochromated $\lambda = 0.710$ 69 Å)	
$\theta$ range, deg	$2.5 < \theta < 24.0$	$2.5 < \theta < 22.7$
no. of indep data coll	6053	6058
no. of obsd. reflns ( $n_h$ ) ( $ F_o  > 3.5\sigma( F )$ )	3951	2669
transmission coeff	0.5688–1.5402	n.a.
$R^a$	0.065	0.083
$R_w^a$	0.086	0.106
GOF	2.291	2.495

$$^a R = \sum(|F_o - (1/k)F_c|)/\sum|F_o|; R_w = [\sum w(F_o - (1/k)F_c)^2/\sum w|F_o|^2]^{1/2}$$

where  $w = [\sigma^2(F_o)]^{-1}$ ;  $\sigma(F_o) = [\sigma^2(F_o^2) + I^4(F_o^2)]^{1/2}/2F_o$ .

The structures were solved by a combination of Patterson and Fourier methods and refined by full-matrix least-squares<sup>18</sup> (the function minimized being  $\sum[w(F_o - (1/k)F_c)^2]$ ). No extinction correction was deemed necessary. The scattering factors used, corrected for the real and imaginary parts of the anomalous dispersion, were taken from the literature.<sup>19</sup>

The contribution of the hydrogen atoms in calculated positions ( $\text{C–H} = 0.95$  Å,  $\text{B(H)} = 1.3\text{B}(\text{C}_{\text{bonded}})$  (Å<sup>2</sup>) was taken into account but not refined. Upon convergence (see Supporting Information Table S1), no significant features were found in the Fourier difference maps of both compounds. The handedness of the structures were tested by refining both enantiomorphs; the coordinates giving the significantly<sup>20</sup> lower  $R_w$  factors were used. Final agreement factors and other relevant data for the refinement are given in Table 3. All calculations were carried out using the Enraf-Nonius MOLEN package.<sup>18</sup>

**Structural Study of **7**.** An empirical absorption correction<sup>21</sup> was applied to the data set by using azimuthal ( $\Psi$ ) scans of three “high- $\chi$ ” ( $\chi > 82^\circ$ ) reflections. Of the 6053 independent data collected, 3951 were considered as observed and used for the refinement. The final full-matrix least-squares refinement cycles were carried out using anisotropic displacement parameters for the ruthenium, phosphorous, and fluorine atoms and for the atoms of the cyclopentadienyl and MeO moieties. All other atoms were treated isotropically: increasing the number of refined parameters, did not yield a significantly better model.<sup>20</sup>

**Structural Study of **8**.** As mentioned above, only crystals of very unsatisfactory quality could be obtained and used for the data collection, resulting in a poor quality of the structure determination (cf. the limited number of observed reflections and the high values of the esd’s of the refined parameters). A total of 6058 independent reflections were collected of which only 2669 were observed ( $F_o > 3.5\sigma(F)$ ) and used for the refinement.

(18) *MolEN: Molecular Structure Solution Procedure*; Enraf-Nonius: Delft, The Netherlands, 1990.

(19) North, A. C. T.; Philips, D. C.; Mathews, F. S. *Acta Crystallogr.* **1968**, *A24*, 351.

(20) Hamilton, W. C. *Acta Crystallogr.* **1965**, *17*, 502.

(21) *International Tables for X-ray Crystallography*; Kynoch Press: Birmingham, England, 1974; Vol. IV.

(22) *WEB LAB VIEWER, version 1.1*; Molecular Simulation Inc., 1996.

(23) *ALCHEMY III. 3D Molecular Modelling Software*; Tripos Associates, Inc.: St. Louis, MS, 1992.

One of the two tetrafluoroborate anions was found to be highly disordered; therefore, a model was constructed using the strongest peaks of a Fourier difference map. During the refinement, the positional parameters of the fluorine atoms were kept fixed and only their isotropic displacement parameters were allowed to vary. The structure was refined as described above, using anisotropic displacement parameters for the ruthenium, phosphorous, and oxygen atoms; all other atoms were treated isotropically. No significant improvement in the model<sup>20</sup> was obtained by increasing the number of refined parameters.

**Synthesis of 6.** To a solution of Ru(OAc)<sub>2</sub>**2** (55.1 mg, 0.0441 mmol) in 5 mL of CH<sub>2</sub>Cl<sub>2</sub> was added 10 equiv of pyrrole (30.6 μL, 0.44 mmol). After 5 min, 2.1 equiv of HBF<sub>4</sub>·Et<sub>2</sub>O (0.093 mmol, 12.6 μL of a 7.3 M solution in diethyl ether) was added. After 3 h, the reaction mixture was evaporated to dryness, washed twice with 3 mL of hexane, and then redissolved in 5 mL of CH<sub>2</sub>Cl<sub>2</sub>. After washing with water (3 × 4 mL) and drying over MgSO<sub>4</sub>, the solution was filtered through Celite and evaporated to dryness. Washing with 2 mL of hexane and drying in vacuo gave 42 mg (74%) of an orange powder. Anal. Calcd for C<sub>74</sub>H<sub>101</sub>BF<sub>4</sub>NO<sub>2</sub>P<sub>2</sub>Ru: C, 69.12; H, 7.84. Found: C, 68.20; H, 8.15. MS (FAB): found 1198.7 (M<sup>+</sup>), calcd 1198.7. IR (KBr): 1123–1040 cm<sup>-1</sup> (BF<sub>4</sub><sup>-</sup>; s, br). <sup>31</sup>P{<sup>1</sup>H} NMR (CD<sub>2</sub>Cl<sub>2</sub>, 298 K): δ 81.9 (d, 46 Hz), 8.2 (d, 46). <sup>19</sup>F{<sup>1</sup>H} NMR (CD<sub>2</sub>Cl<sub>2</sub>, 298 K): δ -153.6 (s, 25%, <sup>10</sup>B, BF<sub>4</sub><sup>-</sup>), -153.7 (s, 75%, <sup>11</sup>B, BF<sub>4</sub><sup>-</sup>).

**Synthesis of 7.** To a solution of Ru(OAc)<sub>2</sub>**2** (46.1 mg, 0.0369 mmol) in 2 mL of CH<sub>2</sub>Cl<sub>2</sub> was added an excess of CpH (40 μL) and then 2.05 equiv of HBF<sub>4</sub>·Et<sub>2</sub>O (0.076 mmol, 10 μL of a 7.3 M solution in diethyl ether). After 3 h, the reaction mixture was evaporated to dryness, washed twice with 4 mL of hexane, and then redissolved in 4 mL of CH<sub>2</sub>Cl<sub>2</sub>. After washing with water (3 × 4 mL) and drying over MgSO<sub>4</sub>, the solution was filtered through Celite and evaporated to dryness. Washing with 2 mL of hexane and drying in vacuo afforded 46 mg (97%) of an orange powder. Anal. Calcd for C<sub>75</sub>H<sub>101</sub>BF<sub>4</sub>O<sub>2</sub>P<sub>2</sub>Ru: C, 70.13; H, 7.93. Found: C, 70.55; H, 8.45. MS (FAB): found 1197.7 (M<sup>+</sup>), calcd 1197.7. IR (KBr): 1182 cm<sup>-1</sup> (BF<sub>4</sub><sup>-</sup>; s, br). <sup>31</sup>P{<sup>1</sup>H} NMR (CD<sub>2</sub>Cl<sub>2</sub>, 298 K): δ 79.4 (d, 47), 8.2 ppm (d, 47). <sup>19</sup>F{<sup>1</sup>H} NMR (CD<sub>2</sub>Cl<sub>2</sub>, 298 K): δ -153.8 (s, 25%, <sup>10</sup>B, BF<sub>4</sub><sup>-</sup>), -153.9 (s, 75%, <sup>11</sup>B, BF<sub>4</sub><sup>-</sup>).

**Synthesis of 8.** To a solution of Ru(OAc)<sub>2</sub>**2** (62.3 mg, 0.0498 mmol) in 2 mL of CH<sub>2</sub>Cl<sub>2</sub> was added an excess of indole (20 mg, 3.4 equiv, 0.17 mmol) and then 2.05 equiv of HBF<sub>4</sub>·Et<sub>2</sub>O (0.10 mmol, 14 μL of a 7.3 M solution in diethyl ether). After 3 h, the reaction mixture was evaporated to dryness, washed twice with 3 mL of hexane, and then redissolved in 4 mL of CH<sub>2</sub>Cl<sub>2</sub>. After washing with water (3 × 4 mL) and drying over MgSO<sub>4</sub>, the solution was filtered over Celite and evaporated to dryness. Washing with 2 mL of hexane and drying in vacuo afforded 67 mg (92%) of a red powder. The compound could be recrystallized by slow diffusion of hexane into a concentrated CH<sub>2</sub>Cl<sub>2</sub> solution at -20 °C. Anal. Calcd for C<sub>78</sub>H<sub>103</sub>B<sub>2</sub>F<sub>8</sub>NO<sub>2</sub>P<sub>2</sub>Ru: C, 65.82; H, 7.29; N, 0.98. Found: C, 65.53; H, 7.41; 1.07. MS (FAB): found 1250.7 (M<sup>+</sup>), calcd 1248.8. <sup>31</sup>P NMR: component A = 75.4 (d, 46.3 Hz), 7.6 (d, 46.3 Hz); component B = 75.0 (d, 48.4 Hz), 12.8 (d, 48.4 Hz); component C is a very broad doublet centered at ca. 67 ppm and is apparently involved in some form of exchange. Components A and B are thought to be η<sup>4</sup>-complexes. The observed <sup>15</sup>N chemical shifts are all in the relatively narrow region from -250 to -256 ppm (CH<sub>3</sub>NO<sub>2</sub>).

**Acknowledgment.** P.S.P. thanks the Swiss National Science Foundation, the ETH Zurich, and F. Hoffmann-La Roche AG for financial support. A.A. thanks the Italian CNR for support. We also thank F. Hoffmann-La Roche AG for a gift of Biphep ligands and the complex Ru(OAc)<sub>2</sub>**(2)**, as well as Johnson Matthey for the loan of precious metals. Special thanks are due to Dr. Heinz Rügger for the <sup>15</sup>N NMR and Dr. Dario Drommi for experimental assistance.

**Supporting Information Available:** Text giving experimental details, tables for **7** and **8** as their BF<sub>4</sub> salts of positional and isotropic equivalent displacement parameters, calculated positions of the hydrogen atoms, anisotropic displacement parameters, and bond distances and angles, and ORTEP figures showing the entire molecules and the full numbering schemes for **7** and **8** as the BF<sub>4</sub> salt (21 pages). See any current masthead page for ordering information.

OM9707275